Mathematical Modelling and Analysis
Volume 9 Number 4, 2004, pages 299–312
 ISSN 1392-6292

# ON THE COOLING OF A FREE THIN FILM AT THE PRESENCE OF THE VAN DER WAALS FORCES

G. GROMYKO[1], S. TABAKOVA[2], L. POPOVA[3]

[1]*Institute of Mathematics of National Academy of Sciences of Belarus*
Surganov 11, 220072, Minsk, Belarus
E-mail: grom@im.bas-net.by

[2]*Department of Mechanics, Technical University - Sofia, branch Plovdiv*
25, Zanko Djustabanov, str., 4000 Plovdiv, Bulgaria
E-mail: stabakova@hotmail.com, sonia@tu-plovdiv.bg

[3]*Department of Applied Mathematics and Modeling, University of Plovdiv*
24, Tzar Asen, str., 4000 Plovdiv, Bulgaria
E-mail: lubpop@ulcc.pu.acad.bg

Received August 31, 2004; revised November 11, 2004

**Abstract.** The cooling of a hot free thin viscous film attached to a rectangular colder frame is considered. The film is under the action of capillary and van der Waals forces and is symmetric with respect to a middle plane. The one-dimensional case of the corresponding non-stationary nonlinear thermo–dynamic problem is solved numerically by a finite difference scheme. The numerical results for the film shape, longitudinal velocity and temperature are obtained for different Reynolds numbers, dimensionless Hamaker constants and radiation numbers.

**Key words:** cooling of films, finite–difference method, mathematical modelling

## 1. Introduction

The cooling of thin liquid films is important during some processes, e.g. non-isothermal film dynamics, when the temperature distribution influences the liquid film physical properties, leading to Marangoni convection, or phase changes processes, when the liquid film solidifies (as discussed in [7, 8]).

If the film is very thin (its thickness is less than the critical thickness $10^{-7}-10^{-8}m$), it can rupture under the action of the intermolecular attractive van der Waals forces [4, 9]. The latter forces have destabilizing effect on the

thin film dynamics. In [4] the effect of varying the magnitude of van der Waals forces (through the dimensionless Hamaker constant $A$) on the drainage and rupture of a thin free film is studied. It is shown that if $A = 0.01$ and $Re = 1$, then the van der Waals force is extremely weak and no rupture occurs, while for higher values of $A$ and $Re$ the rupture is observed.

It is also interesting to examine how these intermolecular attractive forces influence the heat and/or mass transfer. In [10] the 2D evolution equations of a planar film dynamics and surfactant distribution are studied numerically in a case of free thin films and films, coating solid surfaces. The surfactants are found to accumulate at the thicker part of the films and to break up at the rupture zones. This result is confirmed in [1] as a special case of a more general 3D model of curvilinear free film dynamics and surfactants transfer. The following special cases of practical interest are also discussed in [1]: closed spherical bubbles, infinite cylindrical films and catenoids. In [11] the dynamics of a film, formed between two surfactant-coated drops approaching each other at constant velocity, is studied by using the lubrication theory, when the van der Waals forces are taken into account. It is proved that the surfactant concentration depletes in the film drainage regions.

Previous analysis have taken into account only dynamics and surfactant transfer, while the heat transfer in thin films has been poorly investigated [7, 8]. The solidification of a free thin film in a thermostatic approach is considered in [8]. The 3D problem is reduced to a 2D counterpart because the film is close to a free liquid/solid shell-like body with variable small thickness symmetric to a middle plane.

The current work is an extension of papers [3, 4], here we incorporate the heat transfer into the system describing the dynamics of a free thin film attached to a rectangular frame surrounded by an ambient gas. The film is assumed to be initially hot and it is cooled by conduction, convection and radiation with the colder ambient gas. The film is under the action of capillary and van der Waals forces and is symmetric with respect to a middle plane. The model is based on the evolutionary system, which is derived in [7] for the nonstationary nonlinear thermo–dynamic problem. Its one–dimensional form is solved numerically by a finite difference scheme. Numerical results describing the film shape, longitudinal velocity and temperature are presented for different Reynolds numbers, dimensionless Hamaker constants and radiation numbers.

## 2. Problem Formulation

### 2.1. Energy equation

The fluid is taken as Newtonian viscous liquid with constant density $\rho$, dynamic viscosity $\mu$, surface tension $\sigma$, thermal conductivity $\kappa$ and heat capacity $c$. For the considered problem (as in [3, 4]), the thin liquid film is supposed to be symmetrically attached to a rectangular horizontal frame with a stable

center plane $z = 0$. Although the film media is considered as a fluid continuum, the film is assumed to be thin enough for the intermolecular van der Waals forces to act on it and to neglect the gravity action.

A Cartesian coordinate system $(x, y, z)$, which is connected to the frame $x = \pm a$, $y = \pm b$ $(a \leq b)$, is introduced. The mean thickness of the film $\varepsilon a$ is much smaller than the characteristic length $a$, i.e., $\varepsilon << 1$. Then the film free symmetrical surfaces have positions $z = \pm h/2$, where $h(x, y, t) = O(\varepsilon)$ determines the film shape. Since the film is symmetric with respect to the middle plane $z = 0$, the temperature field is also symmetric $\theta^*(z) = \theta^*(-z)$ and the symmetry condition on $z = 0$ reads [8]:

$$\theta^*_z = 0, \quad \text{for } z = 0\,. \tag{2.1}$$

By using the symmetry assumption, we sought the temperature function $\theta^*(x, y, z, t)$ as an asymptotic expansion

$$\theta^*(z) = \theta_0 + \sum_{k=1}^{\infty} z^{2k}\theta_{2k}, \quad -\frac{h}{2} \leq z \leq \frac{h}{2}\,. \tag{2.2}$$

This form satisfies identically (2.1) and the symmetry assumption.

At the absence of heat sources the energy conservation law for the liquid film is given in the integral form:

$$\frac{d}{dt}\int \rho c\theta^* dv = -\int \mathbf{q}^* \cdot \mathbf{n}\, ds\,, \tag{2.3}$$

where the integration is done over the whole film volume and surface, respectively. Here $\mathbf{q}^*$ is the heat flux and $\mathbf{n}$ the unit outward normal vector to the film surface. The heat flux is supposed to obey the Fourier law, $\mathbf{q}^* = -\kappa\nabla\theta^*$ inside the film and to be due to radiation with ambient on both film free surfaces:

$$\mathbf{q}^* \cdot \mathbf{n} = \beta(\theta^{*4} - \theta_a^4) \qquad at \quad z = \pm h/2, \tag{2.4}$$

where $\beta$ is the radiation coefficient and $\theta_a$ is the ambient temperature.

Integrating equation (2.3) along the film thickness $z \in [-h/2, h/2]$, taking into account (2.2) and (2.4), we obtain the local form of the energy balance equation (see [2, 7, 8]). A leading term of order $O(\varepsilon)$ is given as follows:

$$\rho ch\Big\{\frac{\partial\theta_0}{\partial t} + \mathbf{v}_s \cdot \nabla_s\theta_0\Big\} = \kappa\nabla_s(h\nabla_s\theta_0) + 2\beta(\theta_a^4 - \theta_0^4), \tag{2.5}$$

where $\mathbf{v}_s = (u_0, v_0)$ is the surface film velocity vector and $\nabla_s$ the surface gradient. We note that $(u_0, v_0)$ are the leading order terms in a similar asymptotic expansion as (2.2), but for the longitudinal velocity (see (2.1) in [3]).

### 2.2. Dynamic system

Here we shall recall the dynamic system, which was developed in [3, 4]. It describes the film thickness and surface velocity evolution of order $O(\epsilon)$:

$$\begin{cases} h_t + \nabla_s \cdot (h\mathbf{v}_s) = 0, \\ \rho \dfrac{D\mathbf{v}_s}{Dt} = \dfrac{1}{h}\nabla_s \cdot \hat{\mathbf{T}}, \end{cases} \tag{2.6}$$

where $\hat{\mathbf{T}} = -\mathbf{P} + \mathbf{T}$ is the surface film stress tensor, $\mathbf{P}$ is the pressure tensor

$$\mathbf{P} = -0.5\sigma \left[h\nabla_s^2 h\mathbf{I_s} + 0.5(\nabla_s h)^2\mathbf{I_s} - \nabla_s h \otimes \nabla_s h\right] + 1.5h\phi\,,$$

and the viscous stress tensor $\mathbf{T}$ is given by

$$\mathbf{T} = 2\mu h \left\{ (\nabla_s \cdot \mathbf{v_s})\,\mathbf{I_s} + 0.5\left[\nabla_s \mathbf{v_s} + (\nabla_s \mathbf{v_s})^T\right]\right\}\,.$$

Here $\mathbf{I_s}$ is the identical surface tensor, $\phi = A^{'}h^{-3}/(6\pi\rho)$ is the potential function of van der Waals forces, $A^{'}$ is the Hamaker constant ($A^{'} \sim O(10^{-20}J)$) and $^T$ stands for transposition. Equations (2.6) are obtained after a similar asymptotic analysis of the full Navier-Stokes equations with appropriate boundary conditions on free surfaces of the film.

### 2.3. One dimensional model

If the length of one frame is much bigger than the other one, i.e., $b \gg a$, then the effects in $y$ direction are negligible on the dynamics and cooling, and the thermo–dynamic problem depends only on $(x,t)$. The system (2.5) – (2.6) in its dimensionless form simplifies to:

$$\frac{\partial h}{\partial t} + \frac{\partial}{\partial x}(uh) = 0, \tag{2.7}$$

$$\frac{\partial u}{\partial t} + u\frac{\partial u}{\partial x} = \frac{\varepsilon}{We}\frac{\partial^3 h}{\partial x^3} + \frac{4}{Re\,h}\frac{\partial}{\partial x}\Big(h\frac{\partial u}{\partial x}\Big) + \frac{A}{h^4}\frac{\partial h}{\partial x}, \tag{2.8}$$

$$\frac{\partial T}{\partial t} + u\frac{\partial T}{\partial x} = \frac{1}{Pe\,h}\frac{\partial}{\partial x}\Big(h\frac{\partial T}{\partial x}\Big) + \frac{Ra}{Pe\,h}\big(T_a^4 - T^4\big), \tag{2.9}$$

where $Re = \rho aU/\mu$ is the Reynolds number, $We = ReCa = 2\rho aU^2/\sigma$ the Weber number, $Ca$ the capillary number, $A = A^{'}/(2\pi\rho U^2 a^3\varepsilon^3)$ the dimensionless Hamaker constant, $Pe = RePr = \rho caU/\kappa$ the Peclet number, $Ra = 2\beta a\theta_m^3/\varepsilon\,\kappa$ the radiation number, $\theta_m$ the solidification temperature below which the liquid film becomes solid.

The characteristic scales used to derive system (2.7) – (2.9) are the following: $a$ for length, $U$ for velocity (capillary or viscous), $a/U$ for time, $\varepsilon a$ for film thickness and $\theta_m$ for temperature (here $x$, $t$, $u$ and $T$ are dimensionless).

Since during the derivation of system (2.7) - (2.9) the terms of $o(\varepsilon)$ order have been ignored, then the following inequalities should be valid:

$$Re \le \varepsilon^{-1},\ \ We \le 1,\ \ A \ge \varepsilon,\ \ Pe \le \varepsilon^{-1},\ \ Ra \ge \varepsilon Pe\,.$$

The boundary conditions for $h$, $u$ and $T$ are the following:

$$u(0,t) = u(1,t) = 0, \tag{2.10}$$

$$\frac{\partial T}{\partial x}(0,t) = 0, \quad T(1,t) = T_g, \tag{2.11}$$

$$\frac{\partial h}{\partial x}(0,t) = 0, \quad \frac{\partial h}{\partial x}(1,t) = \tan\alpha, \tag{2.12}$$

where $T_g$ is the dimensionless frame temperature and $\frac{\pi}{2} - \alpha$ is the wetting angle with the frame. The initial conditions are given by:

$$h(x,0) = 1, \qquad u(x,0) = 0, \qquad T(x,0) = T_0, \tag{2.13}$$

where $T_0$ is the dimensionless initial temperature of the film.

The mass conservation of the film during its thinning is expressed as:

$$\int_0^1 (h-1)dx = 0\,, \tag{2.14}$$

its validity is proved by integrating (2.7) and taking into account (2.10).

The non-linear non–stationary problem (2.7) – (2.14) is solved in time till one of the following stop conditions is satisfied:

a) at finite time moment $t = \tau$ a minimum value of $h$ is reached, which corresponds to a stable film shape

$$\lim_{t\to\tau} h(x,t) = h(x), \quad \lim_{t\to\tau} u(x,t) = u(x), \quad \lim_{t\to\tau} T(x,t) = T(x), \tag{2.15}$$

b) at time moment $t = \tau$ the effective critical film rupture thickness is reached, at which the actual film rupture occurs at some point $x_r$

$$h(x_r,\tau) \approx 0, \tag{2.16}$$

c) computations are continued till condition $T(x,\tau) \approx 1$ is satisfied.

We assume that the solution of system (2.7) – (2.14) possesses the required smoothness $u, h, T \subset C^4(\Omega)$ in $\Omega = \{0 \le x \le 1\}$ for $0 < t < \tau$.

## 3. Numerical Scheme

The finite–volume method is used to construct the discrete scheme, which satisfies the mass, momentum, heat flux balances on each control volume and therefore on the whole problem domain.

We define a nonuniform time grid

$$\overline{\Omega_t} = \{t_{j+1} = t_j + \triangle t_j, \quad \triangle t_j > 0, \quad j = 0,\ldots,J_\tau, \quad t_0 = 0, \quad t_{J_\tau} = \tau\}.$$

The space grid is also nonuniform, the adaptation of grid nodes is done dynamically during realization of the algorithm. For more accurate approximation of the boundary conditions we introduce two grids displaced with respect to each other. Functions $u$ and $T$ are defined on the grid

$$\overline{\Omega_x^{u,T}} = \{x_i = i\Delta x, \quad i = 0, \ldots, N+1, \quad x_0 = 0,\ x_{N+1} = 1\},$$

while function $h$ is defined on the grid

$$\overline{\Omega_x^h} = \{x_{i-0.5} = (i - 0.5)\Delta x, \quad i = 1, \ldots, N+1\}\,.$$

In this way the problem will be solved on a staggered space grid.

At each time step notation of discrete functions is simplified and indexes are omitted [5].

Two types of control volumes are used: one for $u$ and $T$, and another for $h$. Control volumes with centers at the grid nodes are applied to discretize equations (2.7) – (2.9).

The difference approximation of (2.7) is obtained integrating it on the control volume $[x_{i-1}, x_i]$

$$h_t + \frac{\Delta M - \Delta M_-}{\Delta x} = 0, \quad i = 1, \ldots, N+1, \tag{3.1}$$

where $\Delta M = \Delta M_i =< h >_i < u >_i$ . The notation $<>$, similarly as in [6], means that the values of $h$ and $u$ are taken on the current cell border. We also use notation

$$\Delta M_i = u_i^+ h_i + u_i^- h_{i+1}, \quad u_i = u_i^+ + u_i^-\,,$$
$$u_i^+ = 0.5(u_i + |u_i|) \geq 0, \quad u_i^- = 0.5(u_i - |u_i|) \leq 0.$$

Summing up (3.1) over the grid $\overline{\Omega_x^h}$ we obtain the equality

$$\sum_{i=2}^{N} h_i \Delta x = 1\,.$$

It approximates the mass conservation equation (2.14) with the accuracy $O(\Delta x)$. If the boundary values $h(0, t_{j+1})$ and $h(1, t_{j+1})$ are found from boundary conditions (2.12), then the equality

$$\sum_{i=1}^{N+1} h_i \Delta x = 1$$

gives $O(\Delta x^2)$ approximation of (2.14).

For some values of parameters, e.g. for large $Re$, which correspond to strong convection dominance, we obtain singular problems with small coefficients at the derivative of the leading order (boundary layer problems). In practice, such problems are characterized by boundary layers, where solutions change very fast. We note that these regions also change in time according to the problem specifics. In order to approximate solutions of such problems, it is necessary to develop special difference schemes.

For approximation of the velocity equation such a scheme have been proposed in [4]. It has a sufficiently good accuracy for small and large velocities. In

our model equation (2.8) has similar features, with the convection or diffusion dominance for different $Re$. For its numerical solution an improved variant of the scheme from [4] is proposed

$$u_{\bar{t}} + \frac{1}{2}(u_{+0.5}u)_{\bar{x}} = (\tilde{\mu}_{+0.5}\, u_x)_{\bar{x}} + \frac{\varepsilon}{We} h_{\bar{x}x\dot{x}} - \frac{A}{3}(h^{-3})_x, \tag{3.2}$$

where $\bar{h} = \frac{1}{2}(h + h_{+1})$,

$$\tilde{\mu}_{+0.5} = \mu_{+0.5} F_B(R_{+0.5}), \quad \mu_{+0.5} = \frac{4}{Re}\frac{h_{+1}}{\bar{h}}, \quad R_{+0.5} = \frac{1}{8}\, Re\, \Delta x\, u_{+0.5}\frac{\bar{h}}{h}$$

and the function $F_B$ is a piecewise linear approximation of $\dfrac{R}{\exp R - 1}$.

The temperature equation also has similar features, when it is solved in the system of equations with dominant convection terms. We propose a discretization, which is constructed using the same principle. Moreover, a restriction connected with physical correctness of the solution is imposed, at least in some simple cases, which occur as particular cases of the considered process. For example, let us consider a heat transfer problem without heat exchange with the ambient gas on boundaries, i.e. we consider thermally isolated film surfaces (there is no source term in (2.9) at $Ra = 0$). Then the temperature of film remains in the limits of the initial temperature and the frame temperature. However, if the radiation with a colder ambient takes place, then the film temperature cannot be less than the ambient temperature.

Such tests have been performed with a few discrete schemes, approximating the considered equation. Taking into account the requirement of the maximum principle for the solution and using experimental results obtained with different discrete schemes, we have selected the following discretization, which is an analogue of the combined scheme and is constructed similarly as in [4]:

$$(hT)_{\bar{t}} + (h_{+1}u_{+0.5}T)_{\bar{x}} = (\tilde{\varphi}_{+0.5}\, T_x)_{\bar{x}} + \frac{Ra}{Pe}\left(T_a^4 - T^4\right), \tag{3.3}$$

where

$$\tilde{\varphi}_{+0.5} = \frac{h_{+1}}{Pe}\, F_B(S_{+0.5}), \quad S_{+0.5} = \Delta x\, u_{+0.5} Pe\,.$$

Integrating (2.9) over the control volume $[0, x_{0.5}]$ and taking into account the boundary condition at $x_0 = 0$, we get the boundary discrete equation:

$$(hT)_{\bar{t},0} + \frac{2}{\Delta x}\, h_1 u_{0.5} T_0 = \frac{2}{\Delta x}\, \tilde{\varphi}_{0.5}\, T_{\bar{x},1} + \frac{Ra}{Pe}\left(T_a^4 - T_0^4\right). \tag{3.4}$$

The iteration process for $h$ and $u$ is described in details in [4], therefore it will not be presented here. The nonlinear system (3.1) – (3.4) is solved by an iterative process, considering $h^{s+1}$ and $u^{s+1}$ as already found:

$$
\begin{cases}
(\overset{s+1}{h}\,\overset{s+1}{T})_{\bar{t},0} + \dfrac{2}{\Delta}\overset{s+1}{h}_{1}\overset{s+1}{u}_{0.5}\overset{s+1}{T}_{0} = \dfrac{2}{\Delta x}\overset{s+1}{\tilde{\varphi}}_{0.5}\overset{s+1}{T}_{\bar{x},1} \\
\qquad\qquad + \dfrac{Ra}{Pe}\big(-4\overset{s}{T}{}_{0}^{3}\overset{s+1}{T}_{0} + T_a^4 + 3\overset{s}{T}{}_{0}^{4}\big)\,, \\
(\overset{s+1}{h}\,\overset{s+1}{T})_{\bar{t}} + (\overset{s+1}{h}_{+1}\overset{s+1}{u}_{+0.5}\overset{s+1}{T})_{\bar{x}} = (\overset{s+1}{\tilde{\varphi}}_{+0.5}\overset{s+1}{T}_{x})_{\bar{x}} \\
\qquad\qquad + \dfrac{Ra}{Pe}\big(-4\overset{s}{T}{}^{3}\overset{s+1}{T} + T_a^4 + 3\overset{s}{T}{}^{4}\big), \quad 1 \le i \le N\,, \\
\overset{s+1}{T}_{N+1} = T_g\,.
\end{cases}
\tag{3.5}
$$

We note that the presented linearization of the source term in (3.3), (3.4) preserves the physical correctness of the solution.

The solution of system (3.5) is found by the Thomas algorithm, which takes into account that matrix of the system is three-diagonal

$$
\begin{cases}
-C_0\overset{s+1}{T}_{0} + B_0\overset{s+1}{T}_{1} + F_0 = 0\,, \\
A_i\overset{s+1}{T}_{i-1} - C_i\overset{s+1}{T}_{i} + B_i\overset{s+1}{T}_{i+1} + F_i = 0, \quad i = 1,\dots,N, \\
\overset{s+1}{T}_{N+1} = T_g
\end{cases}
$$

with

$$
A_i = \frac{\tau}{(\Delta x)^2}\overset{s+1}{\tilde{\varphi}}_{i-0.5} + \frac{\tau}{\Delta x}\overset{s+1}{h}_{i}, \quad B_i = \frac{\tau}{(\Delta x)^2}\overset{s+1}{\tilde{\varphi}}_{i+0.5}\,,
$$

$$
C_i = \overset{s+1}{h}_{i} + \frac{\tau}{(\Delta x)^2}\big(\overset{s+1}{\tilde{\varphi}}_{i-0.5} + \overset{s+1}{\tilde{\varphi}}_{i+0.5}\big) + \frac{\tau}{\Delta x}\overset{s+1}{u}_{i+0.5}\overset{s+1}{h}_{i+1} + \frac{4\tau Ra}{Pe}\overset{s}{T}{}^{3},
$$

$$
F_i = \breve{h}_i\breve{T}_i + \frac{\tau Ra}{Pe}\big(3\overset{s}{T}{}_{i}^{4} + T_a^4\big)\,.
$$

The stability condition of the Thomas method requires the positiveness of the coefficients $A_i$, $B_i$ and $D_i = C_i - A_i - B_i$. It follows from formulas given above, that inequalities $A_i > 0$ and $B_i > 0$ are satisfied unconditionally. The positiveness of

$$
D_i = \overset{s+1}{h} + \frac{\tau}{\Delta x}\big(\overset{s+1}{u}_{i+0.5}\overset{s+1}{h}_{i+1} - \overset{s+1}{u}_{i-0.5}\overset{s+1}{h}_{i}\big) + \frac{4\tau Ra}{Pe}\overset{s}{T}{}^{3}
$$

depends on the change of quantities $\overset{s+1}{h}$ and $\overset{s+1}{u}$ and it can be achieved, for example, by diminishing the time step. The violation of the stability condition leads to some restrictions on time steps. Therefore, in order to obtain the correct solution of the problem, it is necessary to check this condition during computations.

If the iterative process is finished when a relative change of both functions $u$ and $T$ at two successive iterations is less than a given small value, then we have reached the steady thermal and dynamic solutions (2.15).

Condition (2.16) cannot be fulfilled exactly and there exists a critical thickness $h_{cri} > 0$, at which the actual rupture of the film occurs, therefore (2.16) is changed to

$$h(x_r, \tau) = h_{cri}. \tag{3.6}$$

We note that the differential problem becomes singular in the region, where $h$ approaches $h_{cri}$.

## 4. Numerical Results

The film drainage in time and its longitudinal velocity were investigated in [4] by a similar numerical scheme as described here. In [4] the analysis was done for various values of the Reynolds number $Re$ ($1 \leq Re \leq 100$) and dimensionless Hamaker constant $A$ ($0.1 \geq A \geq 0$), when the capillary number $Ca$ and $\varepsilon$ were fixed to $Ca = \varepsilon = 0.01$ ($We$ depended only on $Re$, since $We = 0.01Re$). It is found in [4] that the rupture point $x_r$ moves to the right side from the central symmetry point $x = 0$ towards the frame point $x = 1$ and a "dimple" of the film is formed that enlarges in shape with the growing values of $Re$ and $A$. This means that the inertial forces have a destabilizing effect on the film and lead to its drainage and rupture at $A > 0$. The van der Waals forces also destabilize the film dynamics and accelerate the film rupture.

In the present work we focus on the influence of the inertial and van der Waals forces on the heat transfer, and namely on cooling. Also we consider various radiation magnitudes and study their effect on the cooling process as a whole. The presented numerical results are obtained for constant values of coefficients

$$Ca = 0.01, \quad \varepsilon = 0.01, \quad \alpha = 1.37, \quad Pr = 1\,.$$

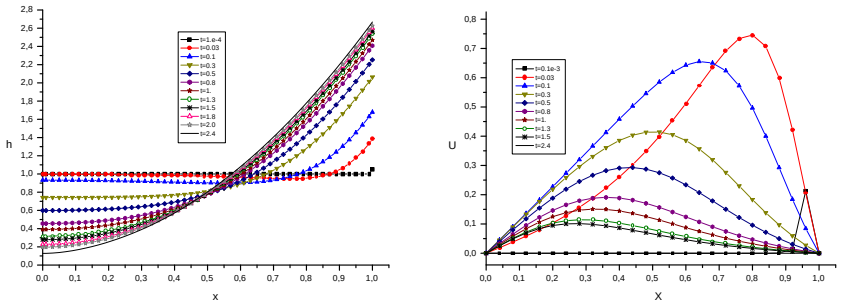


a) b)

**Figure 1.** Evolution in time of functions $h$, $u$ at $A = 0.1$, $Re = Pe = 1$, $We = 0.01$, $T_0 = 1.19$, $T_g = T_a = 1$, $\alpha = 1,37$: a) $h(x,t)$; b) $u(x,t)$.

In Fig. 1 the evolution in space and time of the film thickness $h$, longitudinal velocity $u$ and temperature $T$ are given for the following values of parameters

$$A = 0.1, \quad Re = Pe = 1, \quad We = 0.01, \quad T_0 = 1.19, \quad T_g = T_a = 1.$$

Two different radiation numbers $Ra = 0$ and $Ra = 10$ were used. The rupture of the film is observed at $x = 0$ for a time moment $t = 2.4$ [4].

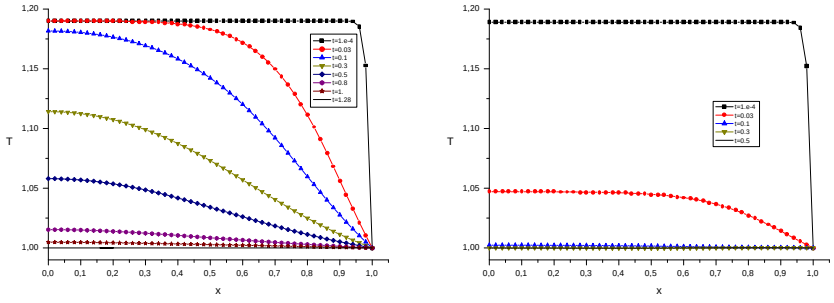


a) b)

**Figure 2.** Evolution in time of the temperature $T$ at $A = 0.1$, $Re = Pe = 1$, $We = 0.01$, $T_0 = 1.19$, $T_g = T_a = 1$, $\alpha = 1,37$: a) $T(x,t)$ at $Ra = 0$, b) $T(x,t)$ at $Ra = 10$.

In Fig. 2 we present results showing dynamics of the temperature. It is seen that the temperature becomes constant and equal to the solidification temperature at different time moments, that are less than the time of rupture. The cooling mechanism is due to convection and conduction in the case of $Ra = 0$ (Fig. 2*a*), while at $Ra = 10$ (Fig. 2*b*) it is dominated by radiation and the larger radiation causes faster cooling. These conclusions are confirmed by additional numerical simulations performed with other values of $Ra$, $T_g$ and $T_a$.

For larger $Re$ ($Re > 1$) the velocity $u$ and the thickness $h$ have large amplitudes and the rupture point moves from the center $x = 0$ towards the frame point $x = 1$. In the case of $Re = 100$, $We = 1$ and $A = 0.1$ the rupture is achieved the time moment $t = 1.757$ in the point $x = 0.53$ [4]. These results are shown in Fig. 3.

In Fig. 4 and Fig. 5 the cooling of the film is presented for the same dynamic parameters and $T_0 = 1.19$, but two different frame and ambient temperature regimes are considered:

a) $T_g = 1$, $T_a = 1$ (see Fig. 4),

b) $T_g = 1.15$, $T_a = 0.9$ (see Fig. 5).

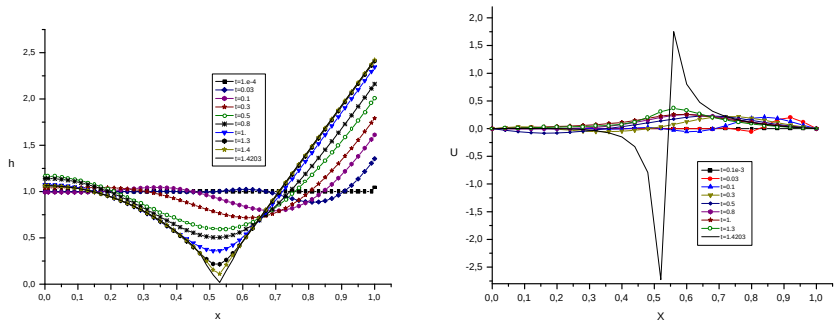


a) b)

**Figure 3.** Evolution in time of functions $h$, $u$ at $A = 0.1$, $\alpha = 1,37$, $Re = Pe = 100$, $We = 1.$, $T_0 = 1.19$, $T_g = T_a = 1$: a) $h(x,t)$; b) $u(x,t)$.

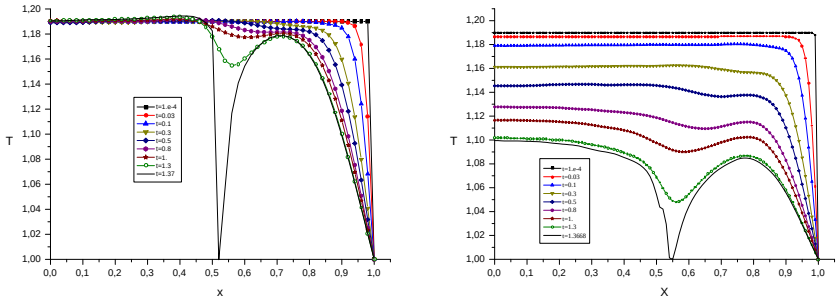


a) b)

**Figure 4.** Evolution in time of $T$ at $A = 0.1$, $\alpha = 1,37$, $Re = Pe = 100$, $We = 1.$, $T_0 = 1.19$, $T_g = T_a = 1$: a) $T(x,t)$ at $Ra = 0$; b) $T(x,t)$ at $Ra = 10$.

Computations are done for radiation numbers $Ra = 0$ and $Ra = 10$. If there is no radiation (Fig.4*a*), then the convection dominates and the temperature profile protrudes towards the point of rupture $x = 0.53$ reaching the solidification temperature $T = 1$ for a time moment smaller than the rupture time, $t = 1.37$.

If the radiation is included, then a cooling of the film till the solidification temperature is accelerated, but the temperature protrusion is visible again (see Fig.4*b* and Fig.5) towards the point $x$ correspondent to the minimum of film thickness at the current time moment, i.e., $x = 0.55$ at $t = 1.3668$ for the first regime and $x = 0.56$ at $t = 1.3245$ for the second regime. The ambient and frame temperature regimes do not have a significant influence on this observation and the only difference is that for $T_g = 1.15$, $T_a = 0.9$ the

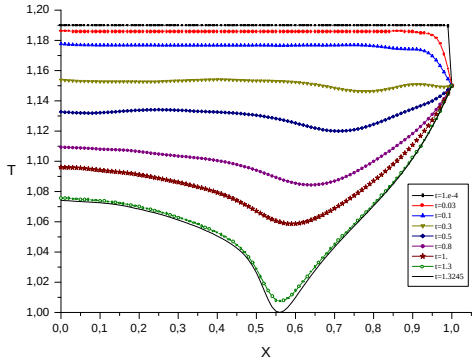


**Figure 5.** Evolution in time of T(x) at $A = 0.1$,$\alpha = 1,37$, $Re = Pe = 100$, $We = 1.$, $T_0 = 1.19$, $T_g = 1.15$, $T_a = 0.9$, $Ra = 10$.

cooling is slightly faster. This can be explained by the the larger value of the radiation term in (2.9).

The temperature profile protrusion tending to break up at the thinner region of the film is confirmed by additional numerical calculations with different frame–ambient temperature regimes and radiation numbers. These results are not given in the present work.

The van der Waals forces have no visible effect on the cooling process, if $Re \leq 1$. The influence of the inertial forces on the convection due to increased $Re > 1$ at the presence of the van der Waals forces is evident when we compare the plots of Fig. 2 with those of Fig. 4. In the latter case the singularity of the dynamic problem is transferred to the thermal problem.

## 5. Conclusions

In the present work we study the cooling of a free thin film attached to a rectangular frame under the action of van der Waals forces. On the basis of the local form of the energy equation derived in [8] and the dynamic equations derived in [3, 4], the 1D nonlinear thermo–dynamic problem is formulated. For its solution, a conservative difference scheme on a staggered space grid is proposed.

Numerical results for the film thickness, its longitudinal velocity and temperature evolution in time are obtained for different Reynolds numbers $Re$ ($1 \leq Re \leq 100$), dimensionless Hamaker constant $A$ ($0 \leq A \leq 0.1$) and radiation numbers $Ra$ ($1 \leq Ra \leq 10$). The following numbers are assumed fixed:

- the capillary number $Ca = \varepsilon = 0.01$, i.e., the Weber number $We = 0.01Re$,
- the Prandtl number $Pr = 1$, i.e., the Peclet number $Pe = Re$.

As a result of the performed numerical analysis, we can make the following *conclusions*:

i) the increase of radiation leads to faster cooling and reaching the solidification temperature before eventual rupture;

ii) the heat convection causes temperature break up in space points corresponding to the thinner film regions, and these times moments are less than or approaching the time moments of film rupture.

The latter conclusion is similar to one obtained for surfactants (mass) transfer, as reported in [2, 10, 11]. Therefore the inertial forces together with the van der Waals forces, which destabilize the film dynamics [4], have the same effect on the temperature field.

The solidification problem, taking into account phase–change conditions (i.e., the Stefan problem) and the film dynamics will be studied in a continuation of the present work.

## References

[1] M.P. Ida and M.J. Miksis. The dynamics of thin films I: General theory; II: Applications. *SIAM J. Appl. Math.*, **58**(2), 456 – 473; 474 – 500, 1998.

[2] P.M. Naghdi. The theory of shells and plates. volume VI a/2, Springer Verlag, Heidelberg, New York, 1974.

[3] L. Popova, G. Gromyko and S. Tabakova. Numerical modeling of free thin film dynamics. *Mathematical Modelling and Analysis*, **8**(1), 291 – 311, 2003.

[4] L. Popova, G. Gromyko and S. Tabakova. Numerical solution of a nonlinear one-dimensional system of differential equations describing the motion of a free thin film. *Differential Equations*, **39**(7), 1037 – 1043, 2003.

[5] A. Samarskii. *Theory of difference schemes.* Nauka, Moskva, 1989.

[6] Yu.I. Shokin and N.N. Yanenko. *Method differential approximation.* Nauka, Novosibirsk, 1985.

[7] S. Tabakova. Solidification of free thin films. *Theoretical and Applied Mechanics*, **30**(2), 39 – 49, 2000.

[8] S. Tabakova and L. Carotenuto. Numerical modeling of the solidification of free thin films. *Microgravity Quarterly*, **4**(1), 55 – 61, 1994.

[9] D. Vaynblat, J. R. Lister and T. P. Witelski. Rupture of thin viscous films by van der waals forces: Evolution and self-similarity. *Phys. Fluids*, **13**(5), 1130 – 1140, 2001.

[10] A. De Witt, D. Gallez and C. I. Christov. Nonlinear evolution equations for thin liquid films with insoluble surfactants. *Phys. Fluids*, **6**, 3256 – 3266, 1994.

[11] L. Y. Yeo, O. K. Matar, E. S. Perez de Ortiz and G. F. Hewitt. Film drainage between two surfactant-coated drops colliding at constant approach velocity. *J. Colloid Interface Sci.*, **257**, 93 – 107, 2003.

**Apie laisvosios plonosios plėvelės atvėsinimą, atsižvelgiant į Van der Valso jėgų poveikį**

G. Gromyko, S. Tabakova, L. Popova

Nagrinėjamas karštosios laisvosios plonosios klampiosios plėvelės, prikabintos prie stačiakampio šaltesnio rėmo, atvėsinimas. Plėvelė yra veikiama kapiliarinių ir Van der Valso jėgų ir yra simetriška vidurio plokštumos atžvilgiu. Atitinkama nestacionari netiesinė termodinaminė problema vienmačiu atveju yra skaitiškai išspręsta baigtinių skirtumų schemos pagalba. Yra gauti skaitiniai rezultatai plėvelės formai, išilginiam greičiui ir temperatūrai skirtingiems Reinoldso skaičiams, bedimensinėms Hamakerio konstantoms ir radiacijos parametrams.